EBioMedicine 66 (2021) 103332

Contents lists available at ScienceDirect

EBioMedicine

journal homepage: www.elsevier.com/locate/ebiom

Research Paper

Metabolomic profiling of pancreatic adenocarcinoma reveals key features driving clinical outcome and drug resistance

Abdessamad El Kaoutari[a,b], Nicolas A Fraunhoffer[a], Owen Hoare[a], Carlos Teyssedou[a], Philippe Soubeyran[a], Odile Gayet[a], Julie Roques[a], Gwen Lomberk[c,d], Raul Urrutia[c,d], Nelson Dusetti[a,*], Juan Iovanna[a,*]

[a] Centre de Recherche en Cancérologie de Marseille (CRCM), INSERM U1068, CNRS UMR 7258, Aix-Marseille Université and Institut Paoli-Calmettes, Parc Scientifique et Technologique de Luminy, Marseille, France
[b] COMPO unit, Inria Sophia Antipolis and CRCM, INSERM U1068, CNRS UMR7258, Aix-Marseille Université UM105, Marseille, France
[c] Genomics and Precision Medicine Center (GSPMC), Medical College of Wisconsin, Milwaukee, WI, USA
[d] Division of Research, Department of Surgery, Medical College of Wisconsin, Milwaukee, WI Center, Medical College of Wisconsin, Milwaukee, WI, USA

ARTICLE INFO

Article History:
Received 3 February 2021
Revised 23 March 2021
Accepted 23 March 2021
Available online xxx

Keywords:
Pancreatic cancer
Metabolomics
Chemosensitivity
Tumor heterogeneity
Metabolic signature
Precision medicine
FSG67

ABSTRACT

Background: Although significant advances have been made recently to characterize the biology of pancreatic ductal adenocarcinoma (PDAC), more efforts are needed to improve our understanding and to face challenges related to the aggressiveness, high mortality rate and chemoresistance of this disease.
Methods: In this study, we perform the metabolomics profiling of 77 PDAC patient-derived tumor xenografts (PDTX) to investigate the relationship of metabolic profiles with overall survival (OS) in PDAC patients, tumor phenotypes and resistance to five anticancer drugs (gemcitabine, oxaliplatin, docetaxel, SN-38 and 5-Fluorouracil).
Findings: We identified a metabolic signature that was able to predict the clinical outcome of PDAC patients ($p < 0.001$, HR=2.68 [95% CI: 1.5−4.9]). The correlation analysis showed that this metabolomic signature was significantly correlated with the PDAC molecular gradient (PAMG) ($R = 0.44$ and $p < 0.001$) indicating significant association to the transcriptomic phenotypes of tumors. Resistance score established, based on growth rate inhibition metrics using 35 PDTX-derived primary cells, allowed to identify several metabolites related to drug resistance which was globally accompanied by accumulation of several diacy-phospholipids and decrease in lysophospholipids. Interestingly, targeting glycerophospholipid synthesis improved sensitivity to the three tested cytotoxic drugs indicating that interfering with metabolism could be a promising therapeutic strategy to overcome the challenging resistance of PDAC.
Interpretation: In conclusion, this study shows that the metabolomic profile of pancreatic PDTX models is strongly associated to clinical outcome, transcriptomic phenotypes and drug resistance. We also showed that targeting the lipidomic profile could be used in combinatory therapies against chemoresistance in PDAC.

1. Introduction

Pancreatic ductal adenocarcinoma (PDAC) is one of the most aggressive and lethal cancers with a dismal outcome due to many factors including the high heterogeneity of tumors, late diagnosis, and high resistance to chemotherapies. The overall 5-year survival rate is currently around 8% which highly depends on the surgery and stage of disease [1]. For example, a tumor resection combined with adjuvant therapies can increase this rate to 20% [2]. However, only 15 to 20% of patients are potentially resectable at the time of diagnosis [3]. PDAC tumors have been classified commonly into two main subtypes, classical, with a better prognosis, and basal-like with a poorer clinical outcome [4,5]. However, the heterogeneity in PDAC tumors is higher than anticipated as shown in recent studies which indicate that not only basal-like and classical cell populations coexist in the same tumor [6] but, a continuum distribution of phenotypes describing PDAC aggressiveness, rather than a binary system, is present in PDAC subtypes [7]. The high level of heterogeneity in PDAC results from a combination of genetic, epigenetic, and micro-environmental alterations, which is directly related to development of drug resistance. In fact, during treatment, a small subpopulation of cancer cells may be able to metabolize the anticancer drug, thereby developing a resistance that allows them to grow and become the dominant

* Corresponding authors.
E-mail addresses: nelson.dusetti@inserm.fr (N. Dusetti), juan.iovanna@inserm.fr (J. Iovanna).

https://doi.org/10.1016/j.ebiom.2021.103332

Research in context

Evidence before this study

PDAC is the most common cancer of the exocrine pancreas and probably the tumor that has benefited the least from clinical progress in the last three decades. Targeting metabolism of cancer cells gives a precious opportunity to overcome challenges related to the high mortality and chemoresistance in PDAC. A limited number of studies concerning metabolomics characterization have been reported on PDAC probably due, at least in part, to the limited access to relevant models.

Added value of this study

Metabolic profiling of PDAC patient-derived tumor xenografts used in this study allowed highlighting the strong link between metabolism and both clinical outcome of the patients and chemoresistance. Metabolic signature was able to discriminate between good and bad prognosis groups of patients based on their level of key metabolites. Identification of key metabolic markers associated to chemoresistance allowed to improve sensitivity to anticancer drugs.

Implications of all the available evidence

These results provide new insights to help to predict patient survival and elaborate new combinatory therapies against chemoresistance in PDAC patients attesting of the important clinical value of this work.

population. This resistance to therapeutic molecules, either intrinsic or newly developed, is still the major challenge in PDAC treatment [8]. Indeed, investigations on the mechanisms underlying drug resistance over the past decade have contributed toward the better understanding of this disease, but more knowledge is needed to improve PDAC chemotherapy.

The metabolic activities in cancer cells are reprogrammed to meet the need of tumors for growth and rapid proliferation through increased biosynthesis and metabolism of macromolecules, such as lipids and amino acids [9–12]. Therefore, given that metabolism is a key regulator of tumorigenesis, therapeutic efficacy is related to the ability to modulate the metabolic alterations of tumor cells. As recently reported, metabolic alterations have been associated with drug resistance in cancer cells [13]. In PDAC, the inhibition of fatty acid biosynthesis is able to overcome gemcitabine resistance [12]. Furthermore, other studies have shown that the oxidative phosphorylation (OXPHOS) pathway in mitochondria significantly contributes to drug resistance. In fact, chemotherapy resistance was associated to high OXPHOS status in several cancers [14,15]. Targeting high OXPHOS in PDAC tumors is synergistic with gemcitabine treatment [16], and disrupting lipid-rafts sensitizes resistant pancreatic tumor initiating cells to standard chemotherapy and decreases their metastatic potential [17]. Hence, therapeutic strategies based on the modulation of metabolism in combination with chemotherapeutic drugs provide a promising opportunity to overcome drug resistance in pancreatic cancer.

In this study, we investigated the metabolic profiles of 77 PDAC PDTXs (patient-derived tumor xenografts) and analyzed their relationship with the resistance to five anticancer drugs to identify relevant metabolic biomarkers. Notably, we found that some metabolites are associated to multidrug resistance, and through modifying the lipidomic profile, we were able to re-senstize PDAC cells to some cytotoxic drugs. Overall, our study reveals key therapeutic targets to improve the treatment of PDAC and overcome drug resistance.

2. Methods

2.1. Ethics statements for Animal and human tissue experiments

The study was approved by the local ethics committee (Comité de protection des personnes Sud Méditerranée I) following patient informed consent (11–61). The PaCaOmics study is registered at www.clinicaltrials.gov with registration number NCT01692873. PDAC samples were collected from Jannuary 2012 to December 2015. All experimental protocols were carried out in accordance with the Guide for the Care and Use of Laboratory Animals (National Academies Press, 2011). All experimental procedures on animals were approved by the Comité d'éthique de Marseille numéro 14 (C2EA-14). Mice were kept within the Experimental Animal House of the centre de Cancérologie de Marseille (CRCM).

2.2. Metabolite extraction

Seventy-seven pancreatic cancer PDTX were obtained as previously described [18] from PaCaOmics clinical trial patients through subcutaneous implantation of PDAC samples into 6-week old male Swiss nude mice (Crl: Nu(lco)–Foxn1nu, Charles River, Wilmington, MA). Both resected PDAC tissue and samples obtained by endoscopic ultrasound-guided fine needle aspiration (EUS-FNA) were fragmented and mixed with 100 μL of Matrigel before subcutaneous injection. The mice tumors were removed after reaching 1.5 cm^3. Then, they were passed three times before proceeding to primary cell culture as described [18].

Endogenous metabolic profiling experiments were measured using mass spectrometry coupled to ultra-performance liquid chromatography (UPLC-MS). Chromatography was performed using an ACQUITY^{TM}HPLC system (Waters Corp., Milford, USA), coupled with the mass spectrometer Waters LCT Premier (Waters Corp., Milford, USA). Due to the wide concentration range of metabolites coupled to their extensive chemical diversity, metabolite extraction was accomplished by fractionating the pancreatic tissue samples into pools of species with similar physicochemical properties, using appropriate combinations of organic solvents as recently described [19]. Thus, multiple UPLC-MS based platforms were used to analyze endogenous metabolic profile for the extraction of the metabolites [19]. Briefly, four separate UPLC-MS plataforms were used to extract and quantify the reported metabolites. PDTX were fractionated into four sections to apply the combination of solvents to extract the specific metabolites group. Methanol and a mix of sodium chloride and chloroform/methanol (2:1) were used to isolate lipids, bile acids, and amino acids. Polar metabolites, including carbon metabolism purification, were done through a mixture of methanol/water (3:2), followed by chloroform and acetonitrile addition. All the measures included three defined quality control samples used to batch normalization.

2.3. Data preprocessing and normalization

Raw data were processed using the TargetLynx application manager for MassLynx 4.1 software (Waters Corp., Milford, USA). A set of predefined retention time, mass-to-charge ratio pairs, Rt-*m/z*, corresponding to metabolites included in the analysis are considered. Associated extracted ion chromatograms (mass tolerance window = 0.05 Da) are then peak-detected and noise-reduced in both the LC and MS domains. A list of chromatographic peak areas is then generated for each sample injection. Normalization factors were calculated for each metabolite by dividing their intensities in each sample by the recorded intensity of an appropriate internal standard in that same sample, following the procedure described by Martinez-

Arranz et al. [20]. Following normalization, sample injection data were returned for manual inspection of the automated integration performed by the TargetLynx software.

2.4. Establishment of drug resistance score

Successful primary cell cultures were derived from 35 PDTX samples with metabolomics data. Thus, PDX samples were split into several small pieces (1 mm3) and processed in a biosafety chamber. After a fine mincing, they were treated with collagenase type V (C9263; Sigma-Aldrich, Inc., St. Louis, Missouri, USA) and trypsin/EDTA (25200−056; Gibco, Sigma-Aldrich, Inc., St. Louis, Missouri, USA) and suspended in DMEM supplemented with 1% w/w penicillin/streptomycin (Gibco, Life Technologies) and 10% of fetal bovine serum (Lonza). After centrifugation, cells were re−suspended in Serum Free Ductal Media (SFDM) and conserved at 37 °C in a 5% CO2 incubator. These cell cultures were seeded in a 96 well plate at a concentration of 5000 cells/well and treated with increasing doses (1 nM to 1 mM) of five different drugs: gemcitabine, oxaliplatin, docetaxel, the active metabolite of Irinotecan SN-38, and 5-fluorouracil (5-FU). Dose-response data were used to calculate the Growth Rate (GR) inhibition metrics using GRmetrics *R* package [21] and to obtain the fitted curves for each drug. Thus, four metrics were considered to establish the GRM (growth rate multimetrics) score, the new score of resistance to drugs based on the following growth rate inhibition metrics: (1) GR50 correspond to the concentration at which the effect reaches 50% of growth rate; (2) GRmax represent the effect at the highest concentration; (3) GR_AOC, refers the area over the curve and (4) The hill coefficient of the fitted curve (h_GR), indicating how steep the curve is. Next, we performed a principal component analysis on these metrics using the FactoMineR [22] package with five dimensions on four GR metrics including GR50, GRmax, GR_AOC and hGR. For each drug, a weighting coefficient was calculated for each metric based on its correlation with PCA dimensions and the corresponding percent of variance as follow: $coeff = \sum_i \left(cor\left(GR\ metric, \dim(i)\right) \times \%variance(i)\right)$.

2.5. Chemograms in presence of FSG67 inhibitors

Four primary PDAC cells (PDAC013T, PDAC017T, PDAC053T and PDAC056T) were cultured in SFDM and plated during 24 h before starting the experiment at 5000 cells per well in a 96-well plate as previously described [23]. Cells were incubated with FSG67 (30 μM), or DMSO as control, 48 h before to start the cytotoxic treatments. A range of concentrations were tested to value to use for the inhibitor. At a concentration of 30 μM we did not found significant cytotoxic effect when FSG67 utilized as single treatment. Cells were then treated with increasing concentrations (1 to 1000 μM) of gemcitabine, oxaliplatin or 5-FU for 72 h in presence or absence of the inhibitor. Cell viability was measured with PrestoBlue (Thermo Fisher Scientific) reagent and quantified using the plate reader Tristar LB941 (Berthold Technologies). Each experiment was repeated at least three times. Values were normalized and expressed as the percentage of the control (vehicle), which represents the 100% of normalized fluorescence.

2.6. Bioinformatics and statistical analysis

All statistical and bioinformatics analysis were performed using different packages and custom scripts of the R programming language. Data were log2 transformed and centered prior to downstream analysis. Hierarchical clustering analysis was performed using ComplexHeatmap library. Independent component analysis (ICA) was performed using JADE package based on five components. Cox proportional hazard regression model from the "*survival*" package was used to perform the univariate survival analysis and determine relative risk of death associated to different factors, with a confidence interval of CI = 95%. Each metabolic feature was associated to the PAMG [7] and drug resistance score using a significant *Pearson's* coefficient of correlation with a p value of correlation test < 0.05. The preprocessing of the data prior to downstream analysis allows to reduce the biais related to the potential extreme values (outliers) which could impact the correlation analysis and thus the biological conclusions.

2.7. Role of funders

The Funders had no role in study design, data collection, data analyses, interpretation, or writing of manuscript.

3. Results

3.1. Metabolic profiling of PDAC

We performed metabolic profiling on 77 pancreatic cancer samples grown as PDTX. Unsupervised clustering analysis of these metabolic profiles revealed distinct clusters on the dendrogram, indicating key heterogeneity among the PDAC samples analyzed. The metabolic heterogeneity across samples was related to the intensity variations in metabolites that belong to different classes as shown in Fig. 1a. Considering the entire metabolome dataset of all samples, a total of 502 metabolites were detected and included in further analysis. The vast majority of these metabolites were from the lipid class. Glycerophospholipids were the most represented class with 45% metabolites followed by glycerolipids (17.1%), fatty acids (10%), sphingolipids (8.2%), amino acids (5.8%), nucleotides (2.8%) and sterols (2.2%), as summarized in Fig. 1b. The other metabolites, representing 9% of all metabolites, included carbohydrates, such as monosaccharides and disaccharides, as well as alkylamines. All metabolite data corresponding to each patient is shown Dataset S1 and the annotation of metabolic feature in Dataset S2. Thus, the metabolomic profiles of human PDAC tumors grown as PDTXs display heterogeneity that is comprised largely of the lipid class of metabolites.

3.2. New metabolic signature to predict patient survival in PDAC

To investigate whether a metabolic profile could impact the survival of PDAC patients, we performed an independent component analysis including all the metabolites, followed by a survival analysis using univariate Cox regression based on PaCaOmics patient cohort [7] to assess their prognostic value. ICA5 component significantly associated with overall survival (OS) in our patient cohort. The weights in this component attributed a score for each sample in the dataset and subsequently used for survival analysis by creating low and high score groups (Fig. 1c). Patient survival in the high-ICA5-score group was significantly improved compared with patients in the low-ICA5-score group with log rank *p-value* < 0.001 and hazard ratio HR = 2.68 (95% CI: 1.5−4.9) (Fig. 1d). These results demonstrated that the metabolic signature identified here has a significant predictive value in OS of patients with PDAC. This predictive value of the metabolic component was then confirmed using a relative risk (RR) regression model. Results showed that patients with lower ICA5 score have significantly higher RR (log rank $p = 0.03$, HR = 0.71 [95% IC: 0.52−0.97]) than patients with higher ICA5 score (Fig. 1e). Clinical features and the ICA5 score of each patient are presented in the Dataset S3.

As described above, the most represented metabolites in the overall patient metabolome belonged to the glycerophospholipid class; however glycerolipids contributed most to the metabolomics signature identified here for predicting patient survival. In Fig. 1f, we represented the top 100 metabolites according to their weights (negative or positive contribution) in component ICA5.

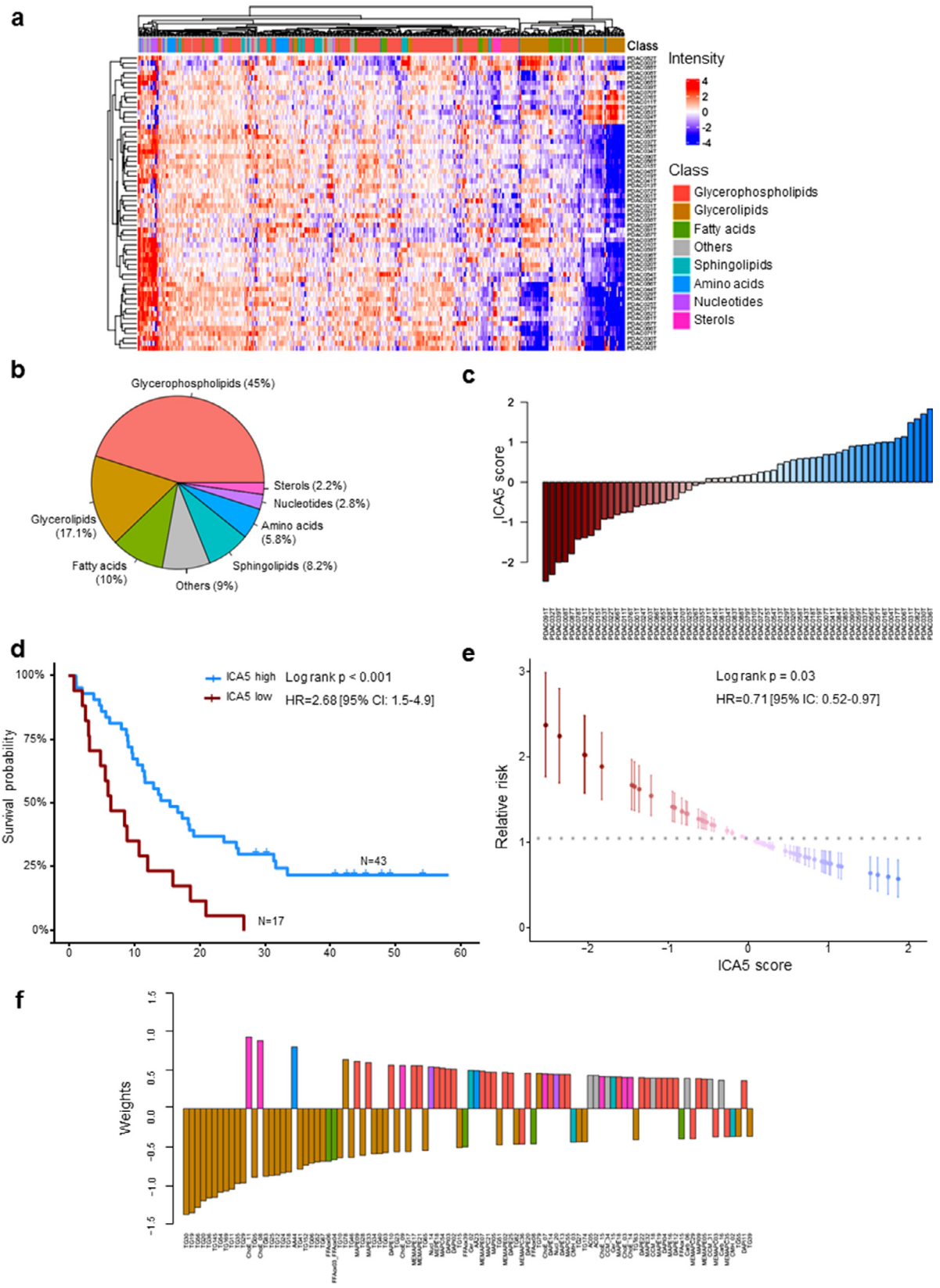

Fig. 1. Metabolic profiling and prognostic signature of PDAC patients. (a) Heatmap showing differential metabolic profiles of PDAC samples using unsupervised hierarchical clustering. The column annotation represents the main classes of metabolites. (b) Pie chart indicating the global distribution of metabolic classes in all samples. (c) Waterfall plot showing the sorted scores of patients in the identified metabolic signatures. (d) Kaplan-Meier plot of survival using univariate analysis based on ICA5 scores of patients. Two groups of patients were considered with high and low score. (e) Univariate relative risk for overall survival associated with the metabolic signature. Each point is a patient's relative risk of disease with error bars corresponding to a 95% confidence interval. (f) Barplot illustrating the contribution of the top 100 metabolites into the component ICA5.

Triacylglycerols, such as TG30 and TG56 along with several oxidized fatty acids, had a negative association to the component suggesting that these metabolites could be associated with poor prognosis. However, cholesteryl esters (ChoE_11 and ChoE_8) and glycerophospholipids, especially lysophospholipids, were positively associated to the component indicating a possible link with improved prognosis in patients with high ICA5 scores (Fig. 1f and Dataset S4). Therefore, component analysis of metabolomic profiles allows us to idenfity key signature associated with patient survival.

3.3. The metabolomics profile associated with phenotype of PDAC

To investigate the link between the metabolomic profiles and molecular phenotypes, we compared the metabolic signature identified in this study with the PDAC molecular gradient (PAMG) previously described [7]. The PAMG is a transcriptomic signature that describes PDAC heterogeneity as a continuous gradient from pure basal-like (low PAMG) to pure classical phenotypes (high PAMG). The correlation analysis showed that the metabolic signature identified in this study significantly correlated with the PAMG with a *Pearson* coefficient $R = 0.44$ and $p < 0.001$ (Fig. 2a and b), indicating the association between the metabolic signatures and transcriptomic phenotypes of the tumors. To note, this comparison was done on the PDTX samples for which the PAMG was available (sixty patients) in the previously published work by Nicolle et al. using the same identification numbers [7]. Along with their good prognosis estimation, tumors with high ICA5 scores appeared to be more classical, while tumors with low ICA5 scores were characterized by a basal-like phenotype with poor prognosis. These results show that the metabolic signature identified here is strongly associated with both tumor phenotypes and OS of patients in PDAC. Furthermore, we performed correlation analysis to identify all metabolites that could be associated individually with the PAMG. Globally, out of 502 metabolic features analyzed, 97 positively correlated with the PAMG and were mainly glycerophospholipids (70%), while 88 metabolites negatively correlated and belonged mainly to glycerolipids (Fig. 2c). For instance, lyso-phosphatidylcholines (LPC) and lyso-phosphatidylethanolamine (LPE), which are part of the glycerophospholipids class, correlated positively to the PAMG, whereas triacylglycerols (TAGs), which are classified as glycerolipids, such as TG73 and TG68, were inversely correlated with the PAMG. As much as 65% of the negatively-correlated metabolites were glycerolipids, followed by glycerophospholipids (15%), in particular 2-acyl-glycero phosphatidylcholine (MEMAPC), and sphingolipids (12.5%) as presented in Fig. 2c). Overall, these results display the strong association between transcriptomic heterogeneity and the metabolic heterogeneity in PDAC patients. We conclude that the more basal-like a tumor is the higher likelihood it exhibits increased levels of fat lipids, such triacylglycerols, as opposed to a classical tumor that would be more prone to present with an accumulation of glycerophospholipids, such as LPC and LPE. The increased level of TAGs in basal-like tumors could be characteristic of tumor aggressiveness, as these fat lipids are the main components of lipid droplets that constitute an important reservoir of fatty acids and energy for cell growth and proliferation.

3.4. Establishment of drug resistance score

To explore the association between the metabolic profiles and drug resistance, we established a new score of resistance based on GR inhibition metrics as described in the methods section. In fact, traditional dose-response metrics such IC50 and Emax could be confounded by the number of cell divisions and the assay duration which induces bias to biological effect of the drug [21]. Using GR metrics fitted to sigmoidal curves allowed thereby a better quantification of the response to drugs. Dose-response data of 35 primary cell lines derived from pancreatic PDTX samples were used to calculate metrics for five drugs tested in this study including gemcitabine, oxaliplatin, docetaxel, SN-38 and 5-fluorouracil (5FU) (Fig. 3a). For each drug, after performing principal component analysis (PCA), a weighting coefficient was calculated for each metric based on its correlation to the first three dimensions that explain more than 90% of variance in the dataset (Supplementary Figs. S1 to S5). To standardize the score calculation, the average weighting coefficient across drugs was used to calculate the GRM score of resistance as follows: GRMs = (log10 (GR50) x GR50Coeff) + (GRmax x GRmaxCoeff) + (GR_AOC x AOCcoeff) + (hGR x hCoeff). It is important to note that all used metrics have positive coefficients except AOC, which is negatively associated to other metrics and had negative weighting coefficient. Thus, GR50Coeff = 1.9, GRmaxCoeff = 2, AOCcoeff = −2.25 and hCoeff = 0.72. The GRM scores were then centered and scaled for further analysis. The score of each drug ranked the tumors from the most resistant (highest score) to the most sensitive by considering multiple metrics normalized to growth rate to provide more robust estimation of drug resistance (Fig. 3b to f).

3.5. Identification of metabolic markers associated to drug resistance

As described above, the GRM score allowed the ranking of patients according to gemcitabine resistance (from the most sensitive to the most resistant). To investigate the metabolites associated with gemcitabine resistance, we performed a *Pearson* regression analysis between all the metabolites in the dataset and gemcitabine GRM scores (correlation threshold $p < 0.05$). As shown in Fig. 4a, the majority of identified metabolites belonged to the glycerophospholipid class, such as diacyl-PC (i.e. DAPC47 and DAPC16) and diacyl-PE (i.e. DAPE09), which positively correlated to the resistant score, whereas several monoacyl-PCs (i.e. MAPC16, MAPC07), monacyl-PE (i.e. MAPE31) and monophosphatidylinositols (PI), such as MAPI03, negatively correlated. In these monoacyl-PC or -PE, namely also lyso-PC or lyso-PE (LPC and LPE, respectively), one fatty acid group is removed and a phosphorylcholine or a phosphorylethanolamine moiety occupies a glycerol substitution site. In addition, amino acids, such as aspartic acid (AA13) and aminoadipic acid (AA28), were increased in resistant cells (Fig. 4a and Supplementary Fig. S6). However, we found a significant decrease in sterol metabolites in resistant cells, including the cholesteryl esters (ChoE_13, ChoE_14 and ChoE_17). Finally, sphingolipids, such as ceramids (Cer_02 and Cer_13) and sphingomyelins (SphLip_04, SphLip_04 and SphLip_13), also inversely correlated to gemcitabine resistance (Fig. 4a and Supplementary Fig. S6). Similarly, metabolic features associated to resistance to oxaliplatin were mostly glycerophospholipids. LPC, such as MAPC49 and MAPC45, were particularly low in resistant cells (highly anti-correlated), as opposed to DAPCs (diacyl-PC), including DAPC47 and DAPC09, along with TAGs, such as TG22 and TG26, which were positively associated to oxaliplatin resistance (Fig. 4b and Supplementary Fig. S7). In fact, sterol levels (i.e. ChoE_03, ChoE_07) were low in resistant cells in conjunction with an increase of amino acids, such as aspartic acid (AA13) and hypotaurine (AA26). This metabolite AA26 was also significantly correlated to increasing resistance to 5-FU along with a polyunsaturated fatty acid (FFA29; docosapentaenoic acid) and many diacyl-PC (i.e. DAPC09, DAPC46) and LPE (MAPE34, MAPE38) (Fig. 4c and Supplementary Fig. S8). In contrast, three free fatty acids (FFAs) decreased in resistant cells, including margaric acid (saturated FFA34), eicosenoic acid (monounsaturated FFA38) and oxidized linoleic acid (polyunsaturated FFAox35). Beyond the singular metabolic features associated to drug resistance presented here, our results suggest that the metabolic profile that characterizes drug-resistant cells in PDAC could be similar for both oxaliplatin and gemcitabine.

Correlation analysis was also utilized to identify numerous metabolites that are associated with GRM scores of SN-38, an active analog of irinotecan and docetaxel. Particularly, we found several nucleotides that were highly associated to SN-38 resistance, including uridine

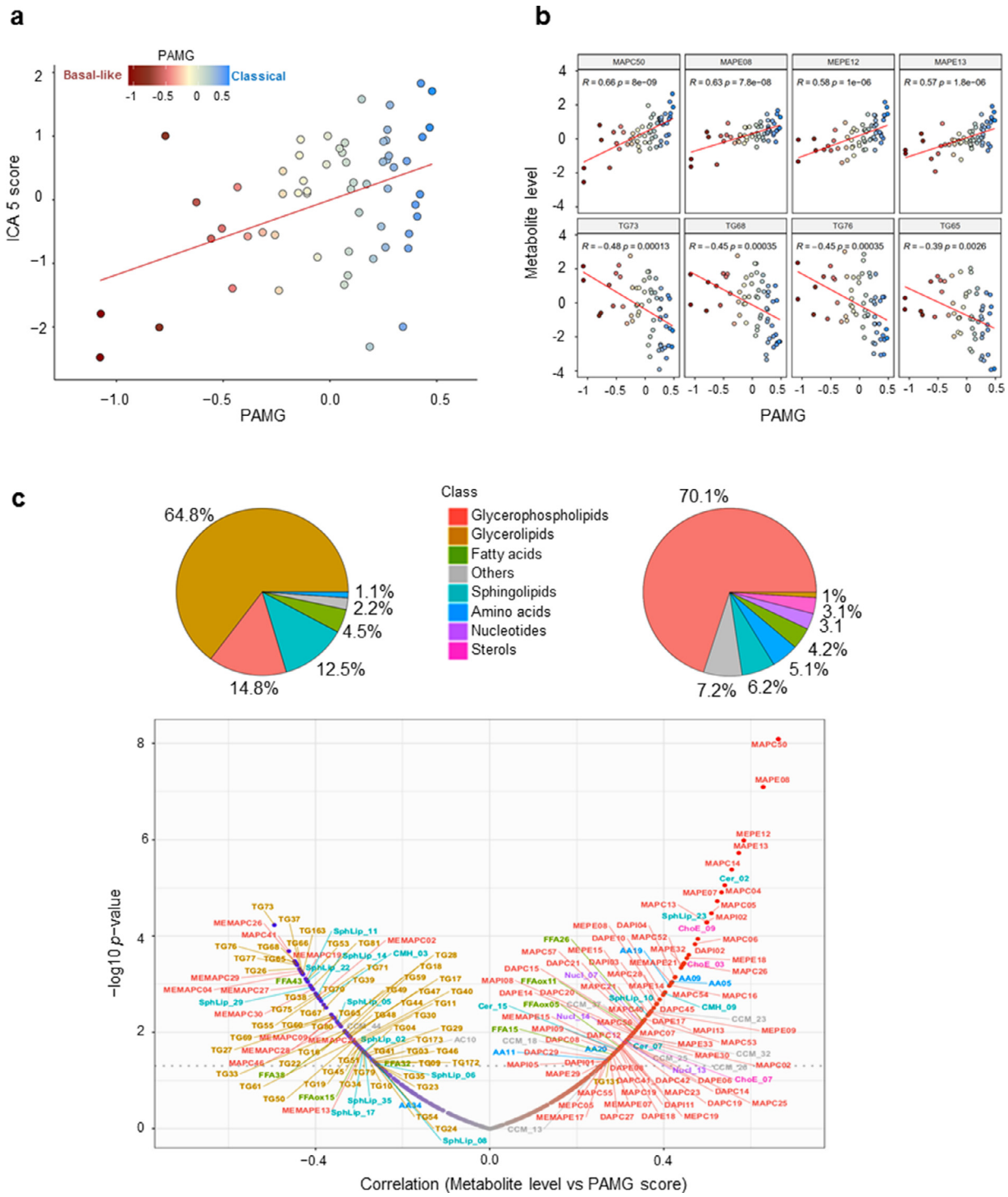

Fig. 2. Metabolic signature is correlated with molecular gradient of the tumors. (a) Scatter plot showing the correlation between molecular gradient and ICA5 scores (*Pearson* coeficient 0.38 and $p = 0.0031$). (b) Scatter plots of most correlated metabolites to molecular gradient. Statistics of the *Pearson's* correlation are shown. (c) Visualization of all correlated metabolic features to molecular gradient. Pie charts and volcanoplot illustrate the repartition among main classes of anticorrelated (left) and correlated (right) metabolites. All metabolites with a *Pearson* correlation p values < 0.05 were shown.

5-monophosphate (a pyrimidine nucleotide Nucl_14), ADP-glucose (purine nucleotides Nucl_22 and Nucl_23), inosine (Nucl_16), guanosine (Nucl_02) and cyclic AMP (Nucl_25) and cytidine monophosphate (Nucl_07), as shown in Fig. 4e. In addition to nucleotides, some LPI, including MAPI08 and MAPI13, and MAPI05, along with a single sphingomyelin (SphLip_25) were positively associated with SN-38 resistance score. In contrast, several sphingomyelins inversely correlated with SN-38 resistance scores (Fig. 4e and Supplementary Fig. S9). Moreover, some PLs, such as diacy-PI DAPI06, diacyl-PE DAPE25 and MEMAPE13 (1-ether, 2-acylglycerophosphocholine), along with acylcarnitines (fatty esters), including L-octanoylcarnitine (AC02), decanoylcarnitine (AC04) and dodecanoylcarnitine (AC05), also had low levels in resistant cells. This data indicates that the metabolic reprogramming related to SN38 resistance results in accumulation of nucleotides in resistant cells, possibly generated by enhanced *de Novo* synthesis.

Regarding metabolic features associated to docetaxel resistance, our results showed increased levels of many sphingolipids, particularly

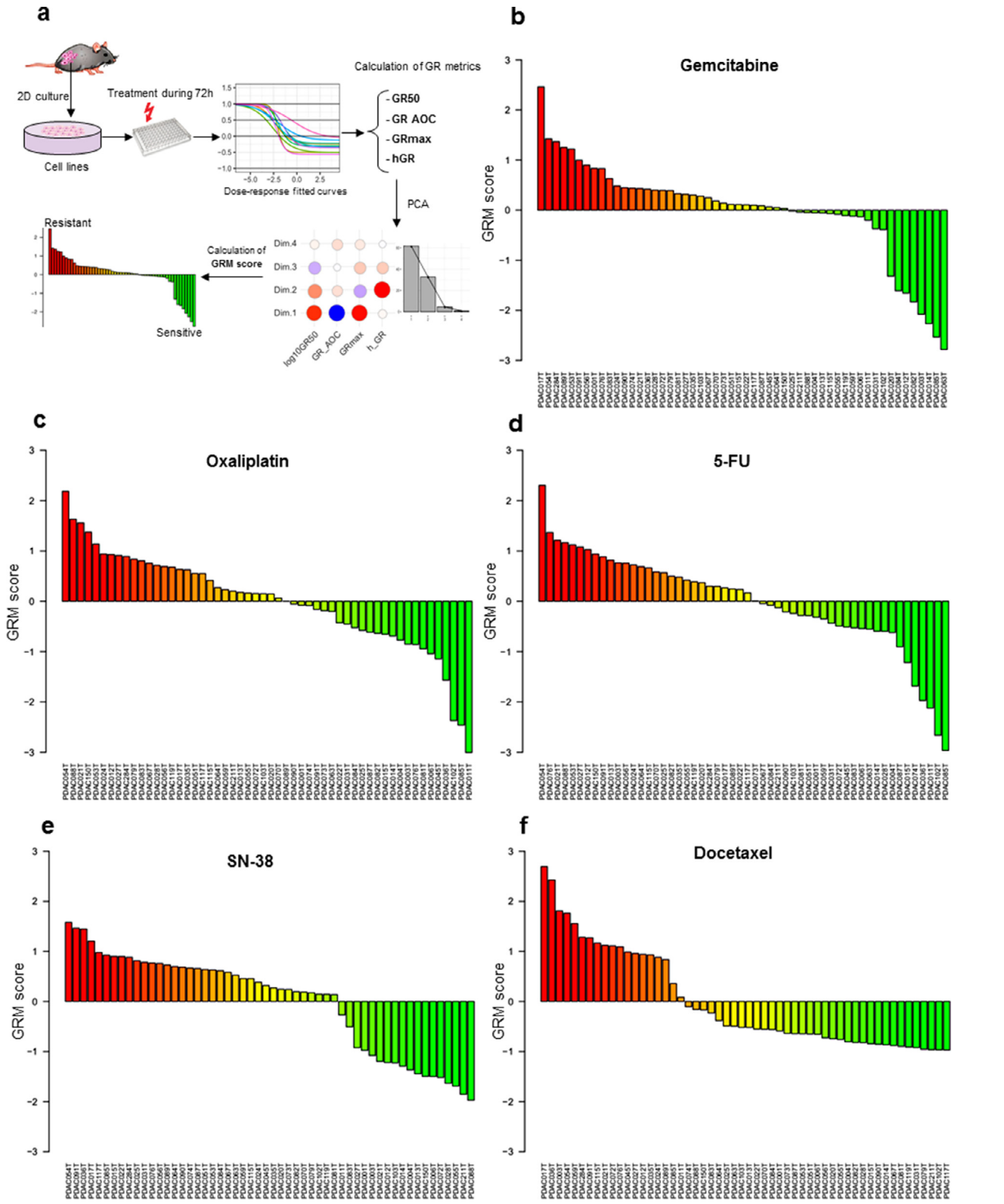

Fig. 3. Establishment of drug resistance score. (a) Schematic illustration of GRM score calculation based on Growth rate fitted curves of dose-response of PDAC cell lines treated with different drugs. (b to f) Ranking of cell lines from the most resistant to the most sensitive based on GRM scores respectively for gemcitabine, oxaliplatin, 5-FU, SN-38 and docetaxel. Red to green colours reflect the gradient of resistance/sensitivity to the drug. Scores were scaled and centered around zero.(For interpretation of the references to color in this figure legend, the reader is referred to the web version of this article.)

ceramides, such as Cer_05, Cer_03 and Cer_09 (Fig. 4e and Supplementary Fig. S10). Eicosenoic acid (FF18) and some LPC, such as MAPC03, MAPC11 and MAPC02, also positively associated with resistance. However, almost all metabolites that negatively correlated to resistance belonged to two main subclasses of phospholipids, namely diacyl-LPE, including DAPE28 and DAPE29, and diacyl-PC, such as DAPC20 and DAPC4 (Fig. 4e and Supplementary Fig. S10). Thus, resistance to docetaxel appears to elicit its own unique metabolic profile. Docetaxel and

paclitaxel are taxanes, they share the same mechanism of action as anticancer agents and show the same score of sensitivity. The difference we found is in their IC50 which is higher for paclitaxel compared to docetaxel. Thus, we consider that using the one or the other is indifferent for scoring sensitivity.

Overall, these results show that the resistance of tumors to chemotherapy treatment is associated to significant changes in metabolic profiles and alteration of several metabolites. These findings provide new insight on the potential of standard chemotherapeutics combined with targeting cancer metabolism as promising treatment strategies for PDAC.

3.6. Multi-drug resistance metabolic features

Our exploration of metabolic features associated to drug resistance identified common metabolites that were significantly correlated in a positive manner to three out of five drugs studied here. Unsupervised clustering based on correlations between GRM scores of each drug and metabolites revealed two distinct main clusters of metabolites, indicating global positive and negative correlations to multidrug resistance (Fig. 5). In fact, gemcitabine, oxaliplatin and 5-FU GRM scores clustered together, highlighting a similar profile of associated metabolites (Fig. 5a and b). Interestingly, we found that phospholipids containing two acyl-groups, such as diacyl-PC and diacy-PE, along with some TAGs could be universally considered as metabolic markers of multidrug resistant (Fig. 5A). In contrast, lysophospholipids and some cholesteryl esters demonstrated a general inverse correlation with multidrug resistance across these three drugs (Fig. 5b and c). These results indicate that PLs, which constitute the major components of the plasma membrane of the cell, could play a key role in the acquisition of multidrug resistance in PDAC tumors.

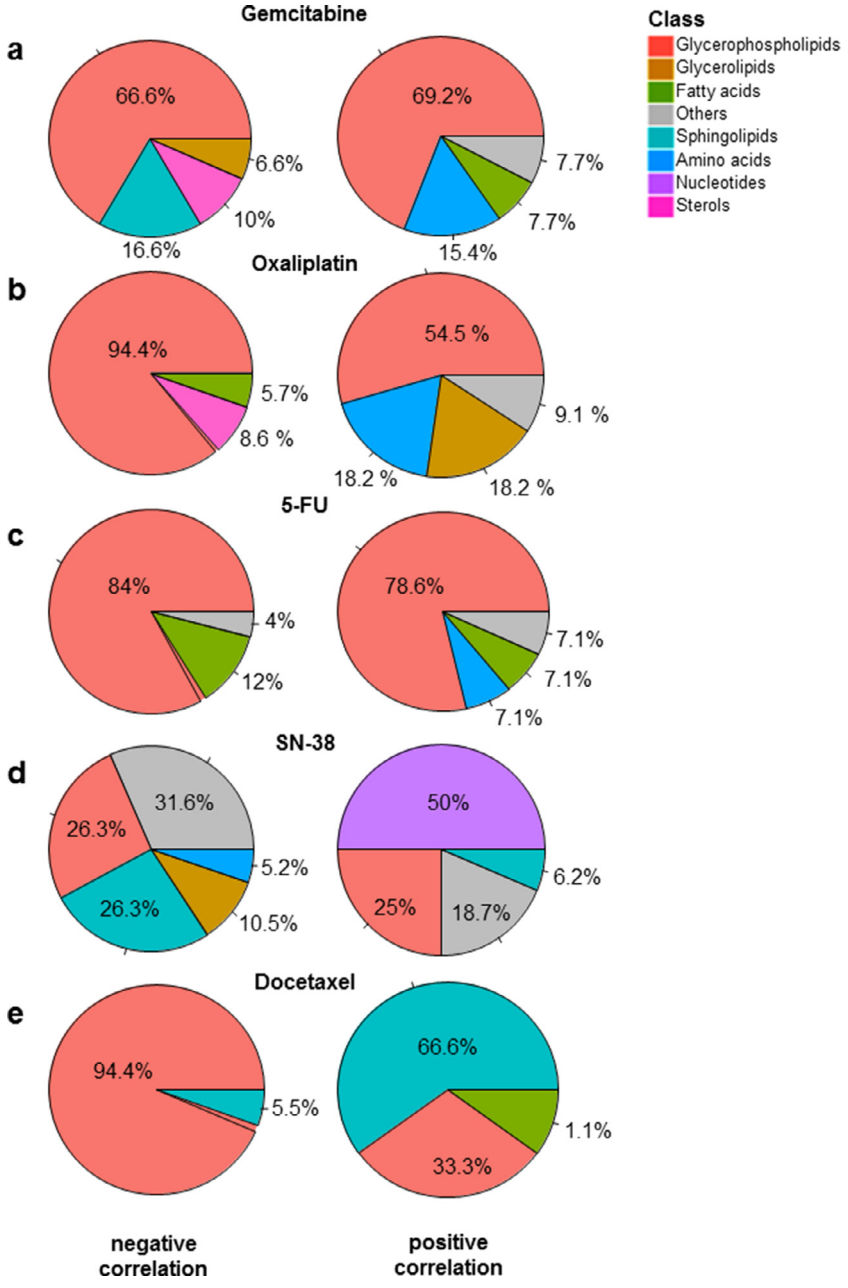

Fig. 4. Metabolic features associated to cytotoxic drugs. Pie charts representing the negative (left) and positive (right) correlated metabolites to the score of resistance to Gemcitabine (a) Oxaliplatin (b), 5-FU (C), SN-38 (d) and Docetaxel (e).

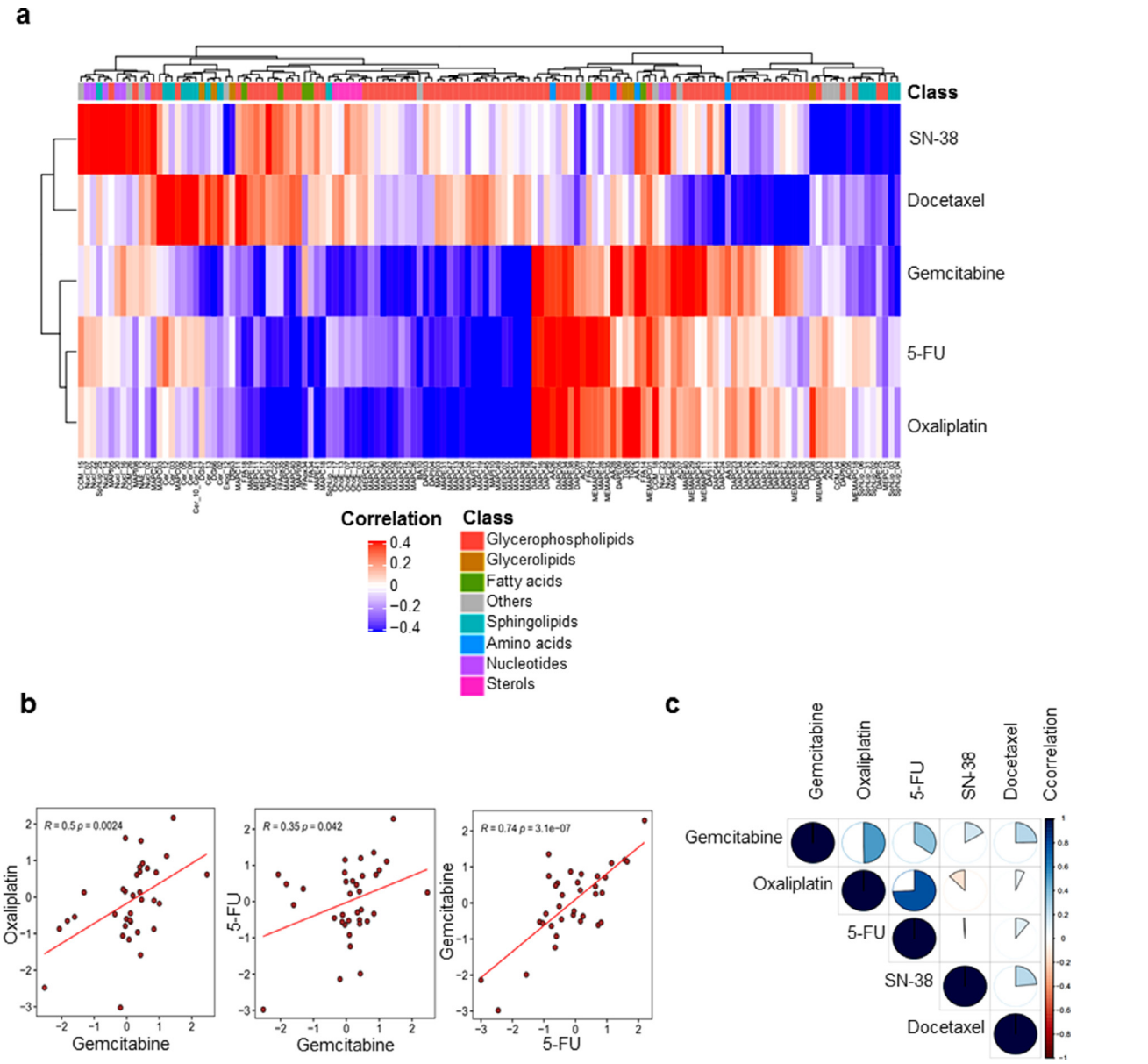

Fig. 5. (a) Heatmap of the hierarchical clustering based on the correlation of all identified metabolic features that were associated to at least one drug. Red and blue colors indicate positive and negative correlation, whereas the white color indicates the absence of correlation. (b) Scatterplots comparing the GRM scores among the three significantly correlated drugs; gemcitabine, oxaliplatin and 5-FU. (c) Graphic visualization of correlation matrix among GRM scores of the five drugs. The proportion of the pie chart indicates the level of correlation and the color indicates positive and negative correlation.(For interpretation of the references to color in this figure legend, the reader is referred to the web version of this article.)

3.7. Targeting the lipid profile for improving chemosensitivity to standard anticancer drugs in PDAC models

Our investigations of associations between metabolic profiles and chemoresistance offer more insights on the metabolic changes related to anticancer drug resistance. As described above, several metabolites belonging to diacyl-PC and TAGs correlated with multi-drug resistance. In particular, glycerophospholipid content positively correlated to multi-drug resistance, indicating a possible role in the acquisition of this cellular phenotype. To understand whether targeting the synthesis of these metabolites could impact the response to chemotherapeutics, we treated primary PDAC-derived cells with increasing concentrations of gemcitabine, oxaliplatin or 5-FU alone or together with the specific inhibitor of glycerol 3-phosphate acyltransferase (GPAT1) FSG67. GPAT1 esterifies acyl-group from acyl-ACP to the sn-1 position of glycerol-3-phosphate, an essential step in glycerophospholipid and triacylglycerol biosynthesis. The GR_AOC in the presence or absence of FSG67 was analyzed (Fig. 6). Remarkably, inhibition of glycerophospholipid synthesis is almost systematically followed by an improved sensitivity to the three cytotoxic drugs tested in several primary cultures. Although more validation experiments are required, these results indicate that the metabolism is a promising therapeutic target to overcome the challenge of chemotherapeutic resistance in pancreatic cancer cells.

4. Discussion

Although several investigations provide an increasing knowledge on the characterization and treatment of PDAC, it remains one of the most lethal diseases with poor prognosis and distinctive chemoresistance development. Many studies have allowed better understanding of the complexity of PDAC tumors, based mainly on molecular

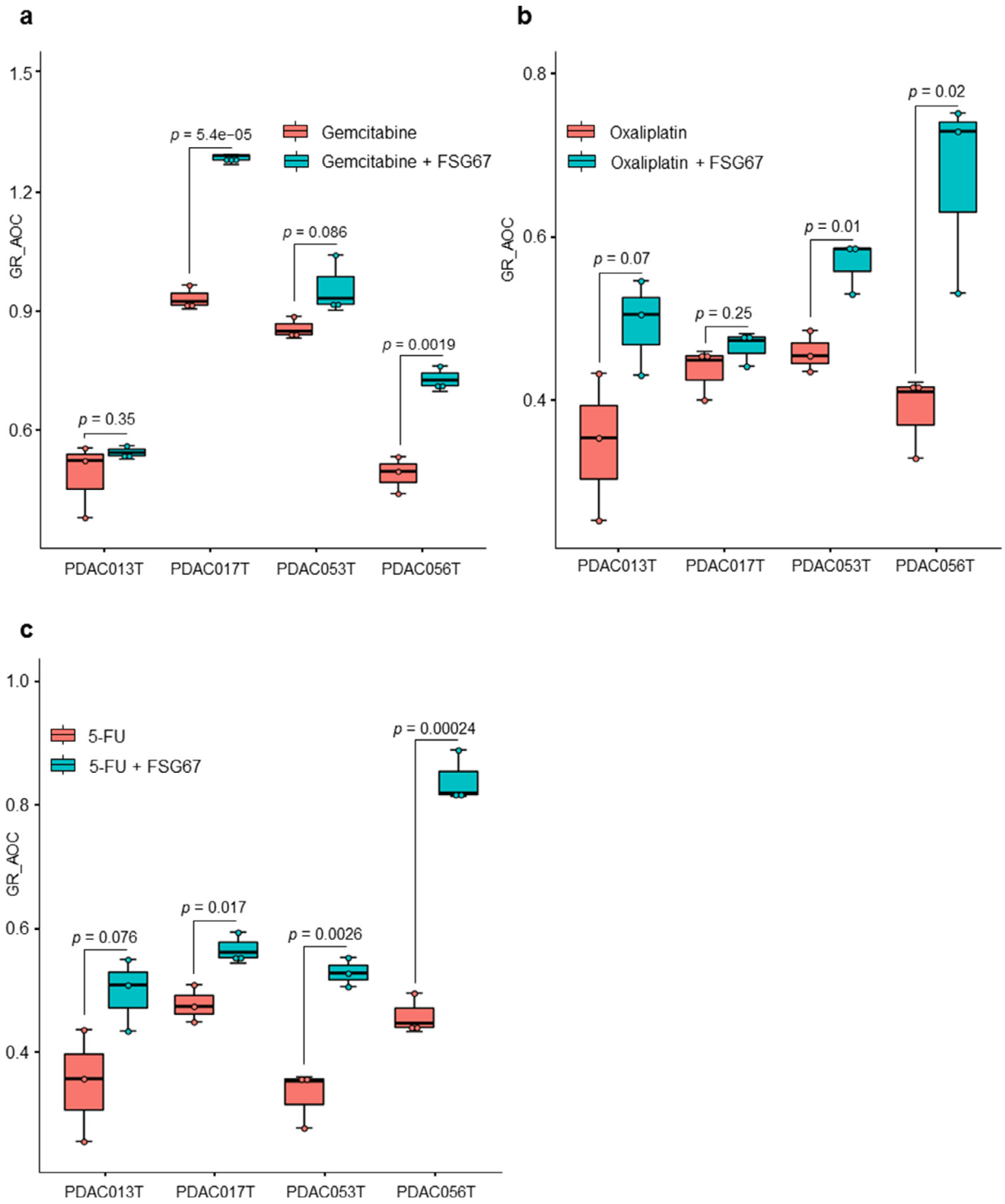

Fig. 6. Effect of FSG67 on treatment with gemcitabine, oxaliplatin and 5-FU. PDAC013T, PDAC017T, PDAC053T and PDAC056T primary cells were treated with increasing concentrations of gemcitabine (a), oxaliplatin (b) and 5-FU (c) in the presence (green) or absence (red) of FSG67. The GR_AOC, represented as boxplots, in the presence or absence of the FSG67 was analyzed.(For interpretation of the references to color in this figure legend, the reader is referred to the web version of this article.)

characterization and classification. PDAC cells demonstrate a significantly reprogrammed metabolism, which facilitates their adaptation to ensure energy and biomass sources for survival and proliferation [9,24]. Thus, in this study, we establish another facet to characterize PDAC tumors at the metabolic level, as a promising area of investigation to offer new insights into the association between PDAC metabolic profiles and their transcriptomic profiles, as well as their resistance to standard chemotherapeutic drugs. Our metabolic profiling of 77 PDTX samples showed that most metabolites were lipids, especially glycerophospholipids and glycerolipids. Unsupervised clustering based on metabolic profiles revealed an important heterogeneity among patients, indicating significant changes in metabolite levels. To characterize this metabolic heterogeneity among tumors, we identified a metabolic signature using ICA analysis. This signature allowed us to, first, draw significant distinctions between patients with worse versus improved clinical outcomes (Fig. 1d and e). This

finding indicates that changes in metabolic features could play a key role in tumor aggressiveness along with patient survival. In addition to its patient prognostic value, the metabolic signature identified here strongly correlated to the PAMG that describes PDAC tumors from the pure basal-like to the pure classical phenotype. PDAC with high ICA5 scores were more classical and characterized by increased levels of glycerophospholipids, while PDAC with low ICA5 scores had a basal-like phenotype with increased levels of triacylglycerols. This result is in concordance with recent studies showing that the accumulation of triacylglycerols correlates with a more aggressive phenotype in lung carcinoma cells [25,26]. Thus, increasing TAG lipolysis in basal-like tumors could be a favorable target to reduce the aggressiveness of tumor cells in which the accumulation of lipid droplets (containing mainly TAGs) constitute an important source of fatty acid and energy for cell growth and proliferation. Moreover, a previous study on PDAC cell lines found a low level of redox metabolites in the glycolytic phenotype, which corresponded with a basal-like cell subtype [27]. Similar results were obtained in our study regarding this subclass of metabolites, which were increased in classical tumors (high ICA5 and high PAMG). In fact, ICA5 scores of PDAC significantly correlated with redox related metabolites, such as CCM_26, which is Flavin adenine dinucleotide (*Pearson* coefficient = 0.37, *p-value* = 0.0032) and CCM_34, a nicotinamide adenine dinucleotide (*Pearson* coefficient = 0.3, *p-value* = 0.018), (Supplementary Fig. S11). These differences in metabolite content, which strongly associate with patient survival and tumor phenotype, demonstrate the key role of metabolic alterations in PDAC cells. In summary, our findings provide additional insights on the characterization of metabolic profiles related to previously identified PDAC phenotypes and clinical outcomes of PDAC patients.

We also investigated the relationship between resistance of PDAC-derived cells to drugs and metabolic profiles. Although studying the synergistic interactions of combining multiple anticancer drugs would be of great interest for clinical application, the goal of this study is to explore the amount of metabolites to different drugs resistance. Our results demonstrated that resistance to cytotoxic drugs associates to a significant imbalance in both type and quantity of metabolic features. Globally, glycerophospholipids seem to be the most altered metabolites between resistant and sensitive tumors, in regards to treatment with the cytotoxic drugs gemcitabine, oxaliplatin and 5-FU. Interestingly, higher resistance was characterized by increased levels of glycerophospholipids, including diacyl-PC and diacyl-PE. Conversely, most of LPC inversely correlated with the resistant score. Previous studies have shown that breast and lung cancer cells are characterized by important quantitative and qualitative alterations of lipid concentrations in the plasma membrane, highlighting the ability to adapt to different environmental conditions to ensure proliferation and survival [28–31]. Moreover, lipid composition of the plasma membrane plays a critical role in the delivery of anticancer drugs to reach their intracellular targets via passive diffusion or active transport [32,33]. One of the mechanisms of drug resistance observed in our study could be related to reduced plasma membrane fluidity in resistant cells. In fact, increased amounts of glycerophospholipids, which constitute major components of the cell membrane, could limit drug diffusion into the cell. Although the mechanistic characterization of drug resistance still very complex, studies reporting the link between modification of plasma membrane composition and anticancer drug resistance are constantly growing [34–38]. In this study, the metabolic features that positively associated to multidrug resistant (at least to gemcitabine, oxaliplatin and 5-FU) were glycerophospholipids, which are constituted by very long chains of fatty acids with the total number of carbon atoms greater than 40. However, down-regulated metabolites, such as LPC, have only one fatty acid chain with a total number of carbon atoms less than 30 (Supplementary Fig. S12). Previously, it has been shown that glycerophospholipids containing very long fatty acyl chains are abundant in the extracellular vesicles derived from gefitinib resistant cancer patients [39]. Here, we employed the GPAT inhibitor, FSG67, to modulate the lipid profile directly on PDAC-derived primary cultures as a proof-of-concept reporting that influencing the lipid content could modulates the therapeutic response to cytotoxic drugs. GPAT1 catalyzes the conversion of glycerol-3-phosphate and long chain acyl-CoA to lysophosphatidic acid (LPA), the rate limiting step in glycerophospholipid synthesis. We found that, in multidrug resistant cells, decreasing the glycerophospholipid synthesis sensitizes the majority of PDAC cells tested here to the effect of three classical cytotoxic drugs (Fig. 6). Indeed, in the present work, we do not focus on the characterization of the mechanistic process of drug development and how targeting potential metabolic markers could reduce the resistance to anti cancer drugs. In fact, the activity of the inhibitor tested here could have a broad impact and lowest specificity due to the high complexity of the metabolic pathways and the high diversity of biosynthesis process that could lead to synthtize a given metabolite. Thus, in the current study, although we observed a significant effect on the drug resistance by using the GPAT inhibitor, our investigations cannot exclude an unspecific effect. Further studies are needed to provide more insights on these aspects to better understanding different interactions between drugs and tumoral cells in PDAC tumors. Moreover, the nature of samples used to study the PDAC tumors is still challenging and need to be taken into account to evaluate the impact of using different pre-clinical models. Here, we used *in vivo* model to perform the metabolic profiling and perform the chemosensitivity assays, when possible, on the corresponding early stage primary cultures to minimize the potential effect of the model and capture the most correct picture of the tumor. Thus, even PDTX models and primary culture cells cannot be generated for 100% of patients due to different factors, the cohort used in this study could be considered as a model representative of PDAC disease with its heterogeneity; including different phenotypes and diverse clinical features.

The recent advances in metabolomics area allowed to improve the extraction and detection of a wide range of metabolites from biological samples. However, more investigations are needed to overcomes the remaining challenges related to the great complexity and diversity of the metabolites which varie widely. In the present study, we used multiple UPLC-MS plateform to capture the highest number of engogenous metabolites in our samples and provide as exaustive as possible picture of the metabolic profile. Moreover, the processing of large amount of metabolomics data is also challenging especially regarding different sources of biais in the datasets and imperfection in the available databases. In this study, we performed several normalization and preprocessing prior to downstream analysis of data to minimize these potential biais and increase the robustness of our conclusions. Also, the use of parametric method to perfom the correlation such as *Pearson* regression allowed better estimation of the linear associations between different variables.

In conclusion, beyond the challenges and limitations discussed above, our findings provide a new insights and add new piece of puzzle to characterize and better understanding the connexions between tumor phenotypes, metabolic profile and resistance to drug in PDAC patients. We also demonstrate that modifying the lipidomic profile by inhibiting the GPAT1 enzyme could be used to improve sensitivity to some cytotoxic drugs, offering a promising therapeutic target to overcome challenges related to drug resistance in PDAC.

Contributors

N.D. and J.I. designed the study. A.EK., N.A.F., O.H., C.T., P.S., O.G., J. R., G.L., and R.U. performed the experiments and analysed the data. A. EK. and J.I. constructed the figures and wrote the manuscript. All authors discussed the results and suggested revisions. A.EK., N.A.F., O.

H., C.T., P.S., O.G., J.R., N.D. and J.I. have full acces to each dataset. All authors read and approved the final version of the manuscript.

Data sharing statement

Data in this study is available upon reasonable request from the corresponding author at juan.iovanna@inserm.fr.

Declaration of Competing Interest

The authors declare no competing interests.

Acknowledgments

We thank Fabienne Guillaumond for critically reading the manuscript. This work is part of the national program Cartes d'Identité des Tumeurs (CIT) funded and developed by the Ligue Nationale Contre le Cancer. This work was supported by INCa (Grants number 2018−078 and 2018−079), Canceropole PACA, Amidex Foundation and INSERM.

Supplementary materials

Supplementary material associated with this article can be found in the online version at doi:10.1016/j.ebiom.2021.103332.

References

[1] Siegel RL, Miller KD, Jemal A. Cancer statistics, 2018. CA Cancer J Clin 2018;68:7–30.
[2] Neoptolemos JP, Palmer DH, Ghaneh P, Psarelli EE, Valle JW, Halloran CM, Faluyi O, O'Reilly DA, Cunningham D, Wadsley J, Darby S, Meyer T, Gillmore R, Anthoney A, Lind P, Glimelius B, Falk S, Izbicki JR, Middleton GW, Cummins S, Ross PJ, Wasan H, McDonald A, Crosby T, Ma YT, Patel K, Sherriff D, Soomal R, Borg D, Sothi S, Hammel P, Hackert T, Jackson R, Buchler MW. European study group for pancreatic, comparison of adjuvant gemcitabine and capecitabine with gemcitabine monotherapy in patients with resected pancreatic cancer (ESPAC-4): a multicentre, open-label, randomised, phase 3 trial. Lancet 2017;389:1011–24.
[3] Hartwig W, Werner J, Jager D, Debus J, Buchler MW. Improvement of surgical results for pancreatic cancer. Lancet Oncol 2013;14:e476–85.
[4] Yachida S, Iacobuzio-Donahue CA. Evolution and dynamics of pancreatic cancer progression. Oncogene 2013;32:5253–60.
[5] Moffitt RA, Marayati R, Flate EL, Volmar KE, Loeza SG, Hoadley KA, Rashid NU, Williams LA, Eaton SC, Chung AH, Smyla JK, Anderson JM, Kim HJ, Bentrem DJ, Talamonti MS, Iacobuzio-Donahue CA, Hollingsworth MA, Yeh JJ. Virtual microdissection identifies distinct tumor-and stroma-specific subtypes of pancreatic ductal adenocarcinoma. Nat Genet 2015;47:1168–78.
[6] Juiz N, Elkaoutari A, Bigonnet M, Gayet O, Roques J, Nicolle R, et al. Basal-like and classical cells coexist in pancreatic cancer revealed by single-cell analysis on biopsy-derived pancreatic cancer organoids from the classical subtype. FASEB J Off Publ Fed Am Soc Exp Biol 2020;34(9):12214–28. doi: 10.1096/fj.202000363RR.
[7] Nicolle R, Blum Y, Duconseil P, Vanbrugghe C, Brandone N, Poizat F, Roques J, Bigonnet M, Gayet O, Rubis M, Elarouci N, Armenoult L, Ayadi M, de Reynies A, Giovannini M, Grandval P, Garcia S, Canivet C, Cros J, Bournet B, Buscail L, Consortium B, Moutardier V, Gilabert M, Iovanna J, Dusetti N. Establishment of a pancreatic adenocarcinoma molecular gradient (PAMG) that predicts the clinical outcome of pancreatic cancer. EBioMedicine 2020;57:102858.
[8] Zeng S, Pottler M, Lan B, Grutzmann R, Pilarsky C, Yang H. Chemoresistance in pancreatic cancer. Int J Mol Sci 2019;20(18):4504. doi: 10.3390/ijms20184504.
[9] Vander Heiden MG, Cantley LC, Thompson CB. Understanding the warburg effect: the metabolic requirements of cell proliferation. Science 2009;324:1029–33.
[10] Cairns RA, Harris IS, Mak TW. Regulation of cancer cell metabolism. Nat Rev Cancer 2011;11:85–95.
[11] Gunda V, Souchek J, Abrego J, Shukla SK, Goode GD, Vernucci E, Dasgupta A, Chaika NV, King RJ, Li S, Wang S, Yu F, Bessho T, Lin C, Singh PK. MUC1-mediated metabolic alterations regulate response to radiotherapy in pancreatic cancer. Clin Cancer Res Off J Am Assoc Cancer Res 2017;23:5881–91.
[12] Tadros S, Shukla SK, King RJ, Gunda V, Vernucci E, Abrego J, Chaika NV, Yu F, Lazenby AJ, Berim L, Grem J, Sasson AR, Singh PK. De novo lipid synthesis facilitates gemcitabine resistance through endoplasmic reticulum stress in pancreatic cancer. Cancer Res 2017;77:5503–17.
[13] Zong L, Pi ZF, Liu S, Liu ZQ, Song FR. Metabolomics analysis of multidrug-resistant breast cancer cells in vitro using methyl-tert-butyl ether method. Rsc Adv 2018;8:15831–41.
[14] Bosc C, Selak MA, Sarry JE. Resistance is futile: targeting mitochondrial energetics and metabolism to overcome drug resistance in cancer treatment. Cell Metab 2017;26:705–7.
[15] Desbats MA, Giacomini I, Prayer-Galetti T, Montopoli M. Metabolic plasticity in chemotherapy resistance. Front Oncol 2020;10:281.
[16] Masoud R, Reyes-Castellanos G, Lac S, Garcia J, Dou S, Shintu L, Abdel Hadi N, Gicquel T, El Kaoutari A, Dieme B, Tranchida F, Cormareche L, Borge L, Gayet O, Pasquier E, Dusetti N, Iovanna J, Carrier A. Targeting mitochondrial complex I overcomes chemoresistance in high oxphos pancreatic cancer. Cell Rep Med 2020;1:100143.
[17] Gupta VK, Sharma NS, Kesh K, Dauer P, Nomura A, Giri B, Dudeja V, Banerjee S, Bhattacharya S, Saluja A, Banerjee S. Metastasis and chemoresistance in CD133 expressing pancreatic cancer cells are dependent on their lipid raft integrity. Cancer Lett 2018;439:101–12.
[18] Duconseil P, Gilabert M, Gayet O, Loncle C, Moutardier V, Turrini O, Calvo E, Ewald J, Giovannini M, Gasmi M, Bories E, Barthet M, Ouaissi M, Goncalves A, Poizat F, Raoul JL, Secq V, Garcia S, Viens P, Iovanna J, Dusetti N. Transcriptomic analysis predicts survival and sensitivity to anticancer drugs of patients with a pancreatic adenocarcinoma. Am J Pathol 2015;185:1022–32.
[19] Simon J, Nunez-Garcia M, Fernandez-Tussy P, Barbier-Torres L, Fernandez-Ramos D, Gomez-Santos B, Buque X, Lopitz-Otsoa F, Goikoetxea-Usandizaga N, Serrano-Macia M, Rodriguez-Agudo R, Bizkarguenaga M, Zubiete-Franco I, Gutierrez-de Juan V, Cabrera D, Alonso C, Iruzubieta P, Romero-Gomez M, van Liempd S, Castro A, Nogueiras R, Varela-Rey M, Falcon-Perez JM, Villa E, Crespo J, Lu SC, Mato JM, Aspichueta P, Delgado TC, Martinez-Chantar ML. Targeting hepatic glutaminase 1 ameliorates non-alcoholic steatohepatitis by restoring very-low-density lipoprotein triglyceride assembly. Cell Metab 2020;31:605–22 e610.
[20] Martinez-Arranz I, Mayo R, Perez-Cormenzana M, Minchole I, Salazar L, Alonso C, Mato JM. Enhancing metabolomics research through data mining. J Proteom 2015;127:275–88.
[21] Hafner M, Niepel M, Chung M, Sorger PK. Growth rate inhibition metrics correct for confounders in measuring sensitivity to cancer drugs. Nat Method 2016;13:521–7.
[22] Le S, Josse J, Husson F. FactomineR: an R package for multivariate analysis. J Stat Softw 2008;25:18.
[23] Fraunhoffer NA, Abuelafia AM, Bigonnet M, Gayet O, Roques J, Telle E, Santofimia-Castano P, Borrello MT, Chuluyan E, Dusetti N, Iovanna J. Evidencing a pancreatic ductal adenocarcinoma subpopulation sensitive to the proteasome inhibitor carfilzomib. Clin Cancer Res Off J Am Assoc Cancer Res 2020;26:5506–19.
[24] Guillaumond F, Leca J, Olivares O, Lavaut MN, Vidal N, Berthezene P, Dusetti NJ, Loncle C, Calvo E, Turrini O, Iovanna JL, Tomasini R, Vasseur S. Strengthened glycolysis under hypoxia supports tumor symbiosis and hexosamine biosynthesis in pancreatic adenocarcinoma. Proc Natl Acad Sci USA 2013;110:3919–24.
[25] Nicolle R, Blum Y, Marisa L, Loncle C, Gayet O, Moutardier V, Turrini O, Giovannini M, Bian B, Bigonnet M, Rubis M, Elarouci N, Armenoult L, Ayadi M, Duconseil P, Gasmi M, Ouaissi M, Maignan A, Lomberk G, Boher JM, Ewald J, Bories E, Garnier J, Goncalves A, Poizat F, Raoul JL, Secq V, Garcia S, Grandval P, Barraud-Blanc M, Norguet E, Gilabert M, Delpero JR, Roques J, Calvo E, Guillaumond F, Vasseur S, Urrutia R, de Reynies A, Dusetti N, Iovanna J. Pancreatic adenocarcinoma therapeutic targets revealed by tumor-stroma cross-talk analyses in patient-derived xenografts. Cell Rep 2017;21:2458–70.
[26] Tomin T, Fritz K, Gindlhuber J, Waldherr L, Pucher B, Thallinger GG, Nomura DK, Schittmayer M, Birner-Gruenberger R. Deletion of adipose triglyceride lipase links triacylglycerol accumulation to a more-aggressive phenotype in A549 lung carcinoma cells. J Proteo Res 2018;17:1415–25.
[27] Daemen A, Peterson D, Sahu N, McCord R, Du X, Liu B, Kowanetz K, Hong R, Moffat J, Gao M, Boudreau A, Mroue R, Corson L, O'Brien T, Qing J, Sampath D, Merchant M, Yauch R, Manning G, Settleman J, Hatzivassiliou G, Evangelista M. Metabolite profiling stratifies pancreatic ductal adenocarcinomas into subtypes with distinct sensitivities to metabolic inhibitors. Proc Natl Acad Sci USA 2015;112:E4410–7.
[28] Cifkova E, Holcapek M, Lisa M, Vrana D, Gatek J, Melichar B. Determination of lipidomic differences between human breast cancer and surrounding normal tissues using HILIC-HPLC/ESI-MS and multivariate data analysis. Anal Bioanal Chem 2015;407:991–1002.
[29] Hilvo M, Denkert C, Lehtinen L, Muller B, Brockmoller S, Seppanen-Laakso T, Budczies J, Bucher E, Yetukuri L, Castillo S, Berg E, Nygren H, Sysi-Aho M, Griffin JL, Fiehn O, Loibl S, Richter-Ehrenstein C, Radke C, Hyotylainen T, Kallioniemi O, Iljin K, Oresic M. Novel theranostic opportunities offered by characterization of altered membrane lipid metabolism in breast cancer progression. Cancer Res 2011;71:3236–45.
[30] Marien E, Meister M, Muley T, Fieuws S, Bordel S, Derua R, Spraggins J, Van de Plas R, Dehairs J, Wouters J, Bagadi M, Dienemann H, Thomas M, Schnabel PA, Caprioli RM, Waelkens E, Swinnen JV. Non-small cell lung cancer is characterized by dramatic changes in phospholipid profiles. Int J Cancer 2015;137:1539–48.
[31] Patterson NH, Alabdulkarim B, Lazaris A, Thomas A, Marcinkiewicz MM, Gao ZH, Vermeulen PB, Chaurand P, Metrakos P. Assessment of pathological response to therapy using lipid mass spectrometry imaging. Sci Rep 2016;6:36814.
[32] Peetla C, Vijayaraghavalu S, Labhasetwar V. Biophysics of cell membrane lipids in cancer drug resistance: implications for drug transport and drug delivery with nanoparticles. Adv Drug Deliv Rev 2013;65:1686–98.

[33] Alves AC, Ribeiro D, Nunes C, Reis S. Biophysics in cancer: the relevance of drug-membrane interaction studies. Biochim Biophys Acta 2016;1858:2231–44.
[34] Bernardes N, Fialho AM. Perturbing the dynamics and organization of cell membrane components: a new paradigm for cancer-targeted therapies. Int J Mol Sci 2018;19(12):3871. doi: 10.3390/ijms19123871.
[35] Blanco VM, Chu Z, Vallabhapurapu SD, Sulaiman MK, Kendler A, Rixe O, Warnick RE, Franco RS, Qi X. Phosphatidylserine-selective targeting and anticancer effects of SapC-DOPS nanovesicles on brain tumors. Oncotarget 2014;5:7105–18.
[36] Brachtendorf S, El-Hindi K, Grosch S. Ceramide synthases in cancer therapy and chemoresistance. Prog Lipid Res 2019;74:160–85.
[37] Comer J, Schulten K, Chipot C. Permeability of a fluid lipid bilayer to short-chain alcohols from first principles. J Chem Theory Comput 2017;13:2523–32.
[38] Kopecka J, Trouillas P, Gasparovic AC, Gazzano E, Assaraf YG, Riganti C. Phospholipids and cholesterol: inducers of cancer multidrug resistance and therapeutic targets. Drug Res Updat Rev Comment Antimicrob Anticanc Chemother 2020;49:100670.
[39] Jung JH, Lee MY, Choi DY, Lee JW, You S, Lee KY, Kim J, Kim KP. Phospholipids of tumor extracellular vesicles stratify gefitinib-resistant nonsmall cell lung cancer cells from gefitinib-sensitive cells. Proteomics 2015;15:824–35.